Dentomaxillofacial Radiology (2018) 47, 20180011

birpublications.org/dmfr

RESEARCH ARTICLE

Metallic materials in the exomass impair cone beam CT voxel values

[1]Amanda P Candemil, [2,3]Benjamin Salmon, [1]Deborah Q Freitas, [4]Glaucia MB Ambrosano, [1]Francisco Haiter-Neto and [1]Matheus L Oliveira

[1]Department of Oral Diagnosis, Division of Oral Radiology, Piracicaba Dental School, University of Campinas, Piracicaba, Brazil; [2]Department of Dental Medicine, Bretonneau Hospital, HUPNVS, AP-HP, Paris, France; [3]EA 2496 - Orofacial Pathologies, Imaging and Biotherapies Lab, Sorbonne Paris Cité - Paris Descartes University., Paris, France; [4]Department of Community Dentistry, Piracicaba Dental School, University of Campinas, Piracicaba, Brazil

Objectives: To assess the influence of artefacts arising from metallic materials in the exomass on cone beam CT (CBCT) voxel values.
Methods: CBCT scans were taken of a phantom composed of 16 tubes filled with a homogeneous hyperdense solution and metallic materials of different compositions (titanium, cobalt–chromium and amalgam) and numbers (one, two and three). The phantom was centred in a 5 × 5 cm field of view such that the metallic materials were located in the exomass, using three CBCT units. Voxel values were obtained from the 16 homogeneous areas and averaged. Also, standard deviation was calculated to measure voxel value variability. Analysis of variance in a factorial scheme with additional treatment 3 × 3 + 3 (material × number + control) was performed, followed by Tukey's test for multiple comparisons, and Dunnett's test for comparisons with the control groups, at a level of significance of 5%.
Results: Metallic material in the exomass significantly reduced the mean voxel value in the CS9300 and Picasso Trio units, and increased voxel value variability in all CBCT units. Amalgam was the material that induced significantly greater reduction of the mean voxel value in the CS9300 and Picasso Trio units, and significantly greater increase in the NewTom Giano. Voxel value variability was significantly greater for amalgam in all conditions. The presence of one cylinder induced significantly less pronounced effects on the mean voxel value and voxel value variability.
Conclusions: Artefacts arising from metallic materials in the exomass have a negative influence on CBCT voxel values.
Dentomaxillofacial Radiology (2018) **47**, 20180011. doi: 10.1259/dmfr.20180011

Cite this article as: Candemil AP, Salmon B, Freitas DQ, Ambrosano GMB, Haiter-Neto F, Oliveira ML. Metallic materials in the exomass impair cone beam CT voxel values. *Dentomaxillofac Radiol* 2018; **47**: 20180011.

Keywords: Cone-beam computed tomography; dental implant; dental alloys; artefacts; in vitro techniques

Introduction

Cone beam CT (CBCT) is an imaging technique that allows for three-dimensional visualization of structures of interest in dentomaxillofacial diagnosis. Compared to multidetector CT (MDCT), CBCT offers some advantages such as higher spatial resolution, lower radiation dose and cost.[1] The scientific literature has demonstrated the great importance of CBCT for dental implant planning, with consistent and accurate evaluation of alveolar bone height, thickness and volume,[2–4] as well as for endodontic,[5] periodontal,[6] orthodontic[7] and oral and maxillofacial surgical treatments.[8,9]

The CBCT image is a matrix composed of small volumetric units known as voxel. Each voxel represents

Correspondence to: Dr Matheus L Oliveira, E-mail: matheuso@unicamp.br
Received 10 January 2018; revised 08 March 2018; accepted 13 March 2018

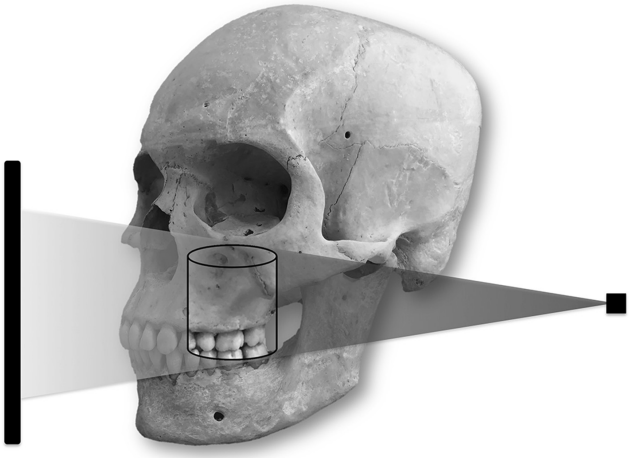

Figure 1 Illustration of a local cone beam CT geometric setting: the cylinder represents the field of view (region of interest), and the triangular shaded area represents the X-ray beam over the exomass.

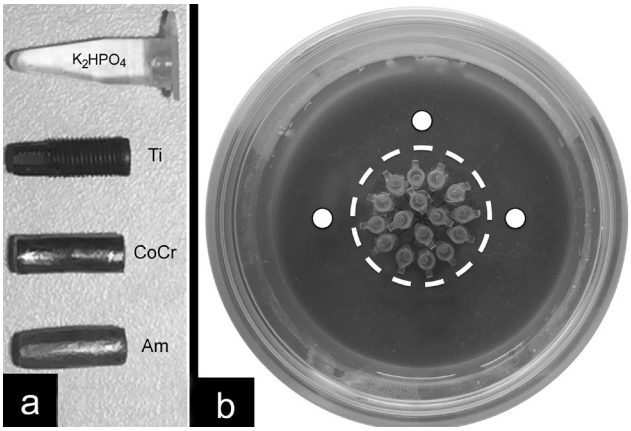

Figure 2 Custom-made exomass phantom: (a) polypropylene tube with K2HPO4 solution, titanium implant (Ti) and cylinders of cobalt–chromium alloy (CoCr) and amalgam (Am); (b) superior view of the container with 16 tubes. The white dotted line indicates the limits of the FOV and the white circles indicate the location of the metallic materials. FOV, field of view; K_2HPO_4, dipotassium phosphate.

the linear attenuation coefficient of inside structure by exhibiting a specific level of grey with a related numerical value (voxel value). More attenuating materials have more hyperdense image with higher voxel values. However, the CBCT voxel values are not accurate due to inherent characteristics of this image modality such as geometric, energetic and computational factors.[10–12] The variability of the voxel values in CBCT contributes to generate artefacts in the reconstructed images,[13–15] which may reduce diagnostic accuracy.[16–18]

It is well-known that an important source of image artefact is the presence of metal objects in the field of view (FOV).[16,17] When the FOV encompasses just a portion of an object which is entirely located in the path of the X-rays (between the focal area and the image detector), this is known as local tomography.[14,19] Moreover, when this phenomenon occurs, any structure that lies outside of the FOV, this constitutes the so-called exomass (Figure 1). In this case, described in the scientific literature as a truncation effect, CBCT image reconstruction attempts to disregard the X-ray attenuation from the exomass to avoid negative interference in the reconstructed image.[20]

Currently, the use of small FOV sizes has increased because of the significant concern of minimizing radiation doses, the need for higher spatial resolution in many diagnostic purposes and the greater accessibility.[21,22] However, smaller FOV sizes result in an indirect increase of the exomass, which has shown to negatively affect the voxel values.[23] Considering the wide use of metallic materials in dentistry associated with the increased indication of small FOV sizes, the objective of this study was to assess the influence of artefacts arising from representative metallic materials in the exomass on CBCT voxel values.

Methods and materials

Custom-made exomass phantom

A thin layer of wax was fixed on the inside bottom of a polypropylene cylindrical container (diameter, 167 mm; height, 65 mm). An aqueous solution of dipotassium phosphate (K_2HPO_4) was prepared at a concentration of 1000 mg ml^{-1} to fill 16 polypropylene tubes of 0.2 ml (Figure 2a). K_2HPO_4 is a salt with high water solubility and density very close to that of calcium hydroxyapatite (2.44 and 3.16 g cm^{-3}, respectively). This concentration was selected to simulate alveolar bone density.[24] The 16 tubes were placed vertically in two concentric circles using a transparent guide that was placed on the wax. The inner and outer circles contained, respectively, 4 and 12 tubes (Figure 2b). To induce the formation of artefacts arising from metallic materials in the exomass, cylindrical metallic materials (diameter, 5 mm; height, 15 mm) of three compositions—titanium implant (KOPP, Curitiba, Brazil), cobalt–chromium alloy (Talmax, Curitiba, Brazil) and silver amalgam (SSWhite, Rio de Janeiro, Brazil; Figure 2a)—could be vertically positioned at the vertices of an imaginary isosceles triangle and at 15 mm from the outer circle of the tubes (Figure 2b). The physical density of the cylinders was calculated based on the Archimedes' principle using an analytical balance discovery (OHAUS Corporation, Parsippany, NJ).[25] Finally, the container was filled with water to simulate the absorption and scattering of the X-rays in soft tissues.

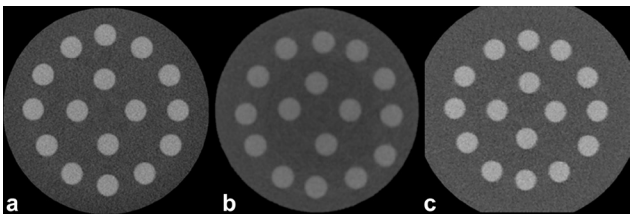

Figure 3 Representative axial reconstructions of the phantom with absence of metallic material in the exomass (control group) obtained with different CBCT units: (a) CS9300; (b) Picasso Trio; (c) NewTom Giano. CBCT, cone beam CT.

CBCT scans

The phantom was placed in the centre of a 5 × 5 cm FOV (diameter × height) such that it could cover all the 16 tubes. Tomographic scans were obtained using three CBCT units: CS9300 (Carestream, Rochester, NY) at 90 kVp, 3.2 mA, exposure time of 20 s, voxel size of 0.09 mm; Picasso Trio (Vatech, Seoul, Republic of Korea) at 90 kVp, 3.0 mA, exposure time of 24 s and voxel size of 0.20 mm; and NewTom Giano (QR, Verona, Italy) at 90 kVp, 3.0 mA, exposure time of 9 s and voxel size of 0.10 mm. All scans resulted in 16 bits images. 10 repeated CBCT scans were obtained of the phantom under the following protocols: control (no metallic material in the exomass); titanium implant (one, two or three titanium implants in the exomass); cobalt–chromium alloy (one, two or three cylinders of cobalt–chromium alloy in the exomass); amalgam (one, two or three cylinders of amalgam in the exomass). When only one metallic material was present in the exomass, it was located in the right region of the FOV. When two materials were present, they were located on both sides of the FOV. When three materials were present, the third one was located in the anterior region of the FOV (Figure 2b). To avoid additional adverse voxel value variability, the three CBCT units were warmed-up (two initial scans) before starting the experiments, and a time interval of 10 min was respected between each acquisition.[26] Figures 3–6 show representative images obtained from each protocol.

CBCT data analysis

Volumetric data from the three CBCT units were reconstructed in their native software programs, exported to Digital Imaging and Communications in Medicine file format and imported into the OsiriX MD imaging software (Pixmeo Sarl, Geneva, Switzerland). From the axial reconstruction of the middle height of the tubes (125 mm above the tip of the tubes), a circular region of interest of 8 mm^2 was selected in the centre of each of the 16 tubes and the voxel values were individually obtained. These values were averaged (mean voxel value) and the standard deviation was calculated to access the variability of CBCT voxel values (voxel value variability) of each CBCT scan. A single examiner assessed all images on a 24.1-inch liquid-crystal display monitor with a resolution of 1920 × 1200 pixels (MDCR-2124, Barco, Kortrijk, Belgium) in a dimly lit, quiet environment. After 60 days, 25% of the sample was reassessed to test intraobserver reproducibility.

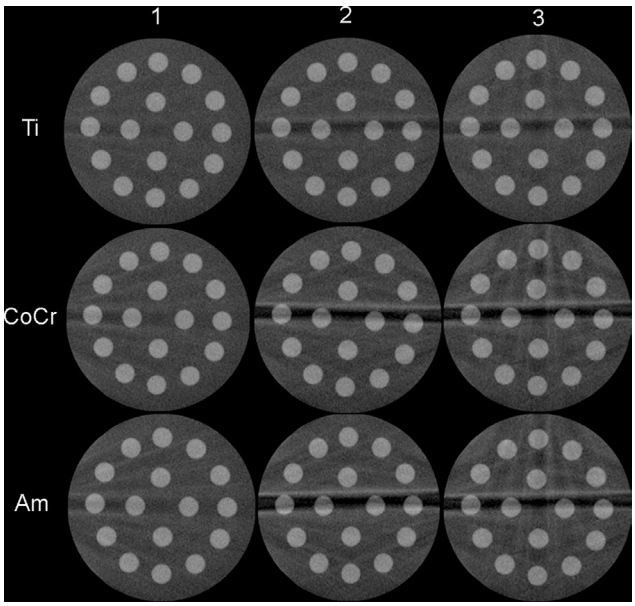

Figure 4 CS9300 CBCT representative axial reconstructions of the phantom with metallic materials in the exomass at different numbers—one, two and three—and compositions—titanium implant (Ti), cobalt–chrome (CoCr) and amalgam (Am). CBCT, cone beam CT.

Analysis of variance in a factorial scheme with additional treatment 3 × 3 + 3 (material × number + control) was performed, followed by Tukey's test for multiple comparisons, and Dunnett's test for comparisons with the control groups. Intraclass correlation coefficient tested the

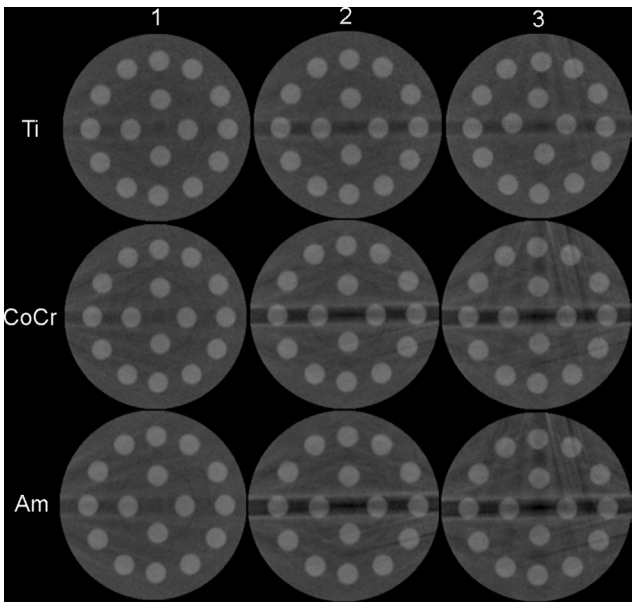

Figure 5 Picasso Trio CBCT representative axial reconstructions of the phantom with metallic materials in the exomass at different numbers—one, two and three—and compositions—titanium implant (Ti), cobalt–chrome (CoCr) and amalgam (Am). CBCT, cone beam CT.

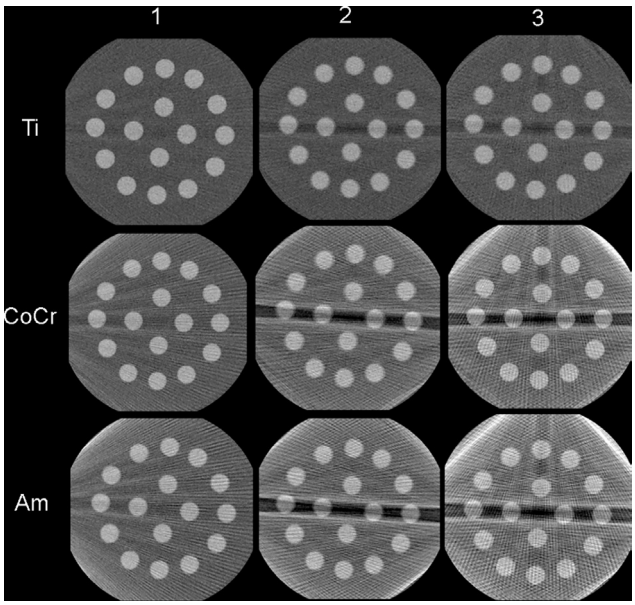

Figure 6 NewTom Giano CBCT representative axial reconstructions of the phantom with metallic materials in the exomass at different numbers—one, two and three—and compositions—titanium implant (Ti), cobalt–chrome (CoCr) and amalgam (Am). CBCT, cone beam CT.

reproducibility of the method. The level of significance was set at 5% ($\alpha = 0.05$).

Results

Intraobserver agreement was 0.99 for both mean voxel values and voxel value variability.

Mean voxel value

As shown in Table 1, the presence of metallic material in the exomass significantly reduced ($p \leq 0.05$) the mean voxel value in all conditions in the CS9300 and Picasso Trio units, and, in the NewTom Giano unit, this significant reduction ($p \leq 0.05$) was observed in the presence of any number of titanium implants and two cylinders of cobalt–chromium or amalgam.

Amalgam had significantly lower mean voxel value ($p \leq 0.05$) in the CS9300 and Picasso Trio units; however, when one cylinder was present no significant difference was observed with cobalt–chromium. In the NewTom Giano, amalgam had significantly higher mean voxel value ($p \leq 0.05$).

The mean voxel value significantly increased ($p \leq 0.05$) in the presence of one cylinder, followed by two and three of any material in the CS9300, of cobalt–chromium and amalgam in the Picasso Trio unit and of titanium in the NewTom Giano unit.

Voxel value variability

Table 2 shows that voxel value variability was significantly higher ($p \leq 0.05$) in the presence of metallic material in the exomass at any number in the three CBCT units.

In the three CBCT units, the voxel value variability was significantly higher ($p \leq 0.05$) for amalgam, which did not differ significantly ($p > 0.05$) from one cylinder of cobalt–chromium in the CS9300, and was significantly lower ($p \leq 0.05$) for titanium, which did not differ significantly ($p > 0.05$) from one cylinder of cobalt-chromium in the Picasso Trio.

The presence of one cylinder led to significantly lower ($p \leq 0.05$) voxel value variability. The presence of two or three cylinders did not differ significantly ($p > 0.05$) between them for cobalt–chromium in the CS9300 and Picasso Trio units, and for any material in the NewTom Giano.

Discussion

The FOV size in CBCT has demonstrated to be one of the most important factors influencing the radiation dose delivered to the patient. Under similar exposure

Table 1 Mean voxel values (standard deviation) in function of the number and composition of materials in the exomass and CBCT units

		Composition		
	Number	*Titanium*	*Cobalt–chromium*	*Amalgam*
CS9300	1	987.73 (4.05)Aa[a]	973.98 (4.03)ABa[a]	959.64 (2.81)Ba[a]
Control	2	950.00 (4.27)Ab[a]	900.15 (17.62)Bb[a]	838.38 (8.22)Cb[a]
1025.87 (3.01)	3	912.33 (4.42)Ac[a]	851.37 (5.70)Bc[a]	777.95 (16.42)Cc[a]
Picasso Trio	1	862.43 (4.89)Aa[a]	839.92 (7.26)Ba[a]	840.84 (4.28)Ba[a]
Control	2	822.18 (12.30)Ab[a]	772.57 (4.41)Bb[a]	748.75 (4.18)Cb[a]
879.73 (5.61)	3	814.25 (4.37)Ab[a]	727.19 (10.84)Bc[a]	689.43 (3.25)Cc[a]
NewTom Giano	1	1356.11 (25.61)Ca[a]	1441.81 (4.14)Ba[a]	1489.08 (11.79)Aa[a]
Control	2	1311.67 (8.11)Cb[a]	1330.03 (17.21)Bb[a]	1367.85 (12.54)Ab[a]
1394.31 (15.67)	3	1280.94 (8.60)Cc[a]	1423.43 (9.93)Ba[a]	1475.59 (11.68)Aa[a]

CBCT, cone beam CT.
[a]Significantly different from the control group. Averages followed by distinct letters (upper case in horizontal and lower case in vertical) differ significantly from each other ($p \leq 0.05$).

Table 2 Mean voxel value variability (standard deviation) in function of the number and composition of materials in the exomass and CBCT units

		Composition		
	Number	*Titanium*	*Cobalt–chromium*	*Amalgam*
CS9300	1	46.58 (1.58)Bc[a]	59.21 (2.51)Ab[a]	63.50 (2.29)Ac[a]
Control	2	80.94 (3.61)Cb[a]	158.82 (5.74)Ba[a]	223.96 (8.36)Aa[a]
39.41 (1.36)	3	94.36 (3.11)Ca[a]	158.60 (4.97)Ba[a]	209.42 (9.38)Ab[a]
Picasso Trio	1	58.46 (1.92)Bc[a]	61.53 (2.34)Bb[a]	66.98 (2.39)Ac[a]
Control	2	93.99 (2.16)Ca[a]	159.64 (2.39)Ba[a]	176.44 (3.11)Aa[a]
52.99 (1.98)	3	84.21 (2.32)Cb[a]	157.83 (2.75)Ba[a]	171.73 (3.30)Ab[a]
NewTom Giano	1	33.48 (2.65)Cb[a]	66.85 (4.47)Bb[a]	85.72 (2.72)Ab[a]
Control	2	92.67 (3.12)Ca[a]	345.90 (9.77)Ba[a]	424.29 (6.42)Aa[a]
24.21 (3.07)	3	95.70 (3.15)Ca[a]	341.26 (5.76)Ba[a]	417.95 (7.42)Aa[a]

CBCT, cone beam CT.
[a]Significantly different from the control group. Averages followed by distinct letters (upper case in horizontal and lower case in vertical) differ significantly from each other ($p \leq 0.05$).

settings, smaller FOV sizes lead to lower doses of X-rays and better theoretical image quality by collimating the primary beam and reducing scattering.[21,22] In 2012, the European project SEDENTEXCT developed evidence-based guidelines on use of CBCT in dentistry and recommended the use of the smallest FOV available on the equipment and consistent with the individual diagnostic task.[9] However, the use of local tomography by reducing the FOV size in the axial plane indirectly increases the exomass impact and the occurrence of truncation effect[19–21,27,28] and inconsistencies in the reconstructed volume.[14] To the best of the authors' knowledge, it seems that the effect of artefacts arising from metal objects in the exomass on CBCT voxel values has not been studied yet. Hence, considering that such inconsistencies may cause general voxel value variability rather than a definite pattern,[14] the current methodology included different CBCT units capable of producing limited scan volumes to better understand this occurrence.

In the present study, metallic materials in the exomass produced noticeable hypodense and hyperdense streaks (Figures 4–6), which are image artefacts resulting from beam hardening and scattering, as well as data extinction.[22,27–29] For instance, mean voxel value reduced (image darkening) in the presence of any metallic material in the exomass in the CS9300 and Picasso Trio, and in the presence of two cylinders of cobalt–chromium or amalgam in the NewTom Giano. This indicates that hypodense artefacts were more predominant in the image and, in a clinical situation, could possibly affect the diagnosis of hypodense conditions, such as fracture lines.

Conversely, in the NewTom Giano, the presence of one or three cylinders of cobalt–chromium or amalgam induced greater formation of hyperdense artefacts. This difference in results observed between CBCT units is probably a consequence of some exposure parameters, such as milliampere-second (mAs), which, although adjusted to be as similar as possible, was not exactly the same. The CS9300, Picasso Trio and NewTom Giano operated at 64, 72 and 27 mAs, respectively, and at 90 kVp. Additionally, since Newtom Giano is equipped with an automatic exposure control system (SafeBeam™ technology), the milliamperage could have been regulated to keep the detector signal constant. CBCT units operating at higher mAs produce more photons of X-rays, which, at the same energy level, may increase the impact of beam hardening-related hypodense artefacts over the whole image. Despite this hypothesis, Oliveira et al did not find a significant influence of milliamperage on voxel value variability.[24]

In the NewTom Giano, the presence of two cylinders of any material induced a reduction of mean voxel value, which could be explained by the arrangement of the cylinders in the exomass. As detailed in the methodology section, even this being a purely *in vitro* study, the cylinders were placed at specific distances at the vertices of an imaginary isosceles triangle to simulate one anterior and two posterior areas of a human mandible. In all CBCT scans, when only two cylinders were present, they were aligned in both sides of the "posterior" region, which induced photon starvation and the formation of an impacting artefact of data extinction. This substantial reduction of mean voxel value showed to be enough to overcome the high voxel values of the hyperdense artefacts. Furthermore, the CS9300, Picasso Trio and NewTom Giano made use of different number of projections (frames), which were 480, 720 and 360, respectively. A reduced data sampling may lead to misregistration, sharper edges and noisier images, because of aliasing, where fine striations appear.[30,31] However, when comparing results of different CBCT units, besides discussing quantitative parameters, possible confidential image reconstruction features should be considered.

It is well-known in the scientific literature that CBCT voxel values are inhomogeneous and do not present a standardized scale.[11] Thus, the imaging phantom used

in the present study was composed of tubes with a radiopaque solution under the same concentration such that the standard deviation of their voxel values could indicate voxel value variability.

The presence of metallic materials in the exomass increased voxel value variability in the three CBCT units is in agreement with previous studies that evaluated the influence on image quality of metallic materials within the FOV.[22,27,29] Oliveira et al showed a reduction of voxel value variability in the presence of a thin and uniform layer of water as the exomass, and they suggest that such a homogeneous exomass should have acted as a filter of the X-ray beam.[24] In the study of Nardi et al metallic materials (*e.g.* orthodontic appliances, osteosynthesis devices, dental implant, prosthetic pin, prosthetic metal structure, endodontically treated tooth and/or prosthetic crown) did not interfere with the image quality.[32] However, these results were subjectively obtained by means of visual assessment.

The presence of only one cylinder of any material in the exomass presented reduced voxel value variability when compared with the presence of two or three cylinders, which may possibly indicate that reduced image deterioration can be expected of patients with fewer metallic objects. The physical properties of an object directly impact the presence/magnitude of artefacts in CBCT. In the present study, amalgam and titanium promoted the highest and lowest voxel value variability, respectively. Considering the similarities in shape and size of the cylinders, this difference should be related to additional physical properties. The atomic number of the titanium is 22 and the density of the cylinder was 4.301 kg m^{-3}. The cylinder of amalgam had a density of 10.153 kg m^{-3}, and the atomic number of the components is mercury-80, silver-47, tin-50 and copper-29. High atomic number and physical density are expected to increase artefact formation when interacting with the X-ray beam.[33,34]

Some scientific studies have shown that reduced CBCT voxel value variability can be expected from larger FOV sizes.[22,27,32,35] However, under similar energetic parameters, it is not justified to indicate larger FOV sizes just to theoretically improve image quality, considering that the patient will be receiving higher dose of X-ray. Instead, priority should be given to understand and, possibly, reduce the effects caused by the exomass. An important limitation of most studies assessing different CBCT units is the inability of standardizing the exposure factors to have all machines operating under the same conditions.

Conclusion

Artefacts arising from metallic materials in the exomass have a significant negative influence on CBCT voxel values. Further studies and technological approaches should consider the impact of exomass on image quality.

Funding

The authors gratefully acknowledge financial support from CAPES-Brazil, Coordination for the Improvement of Higher Education Personnel, and from the International Relations Office (DERI; 26/2016) at UNICAMP.

References

1. Abramovitch K, Rice DD. Basic principles of cone beam computed tomography. *Dent Clin North Am* 2014; **58**: 463–84. doi: https://doi.org/10.1016/j.cden.2014.03.002
2. Bornstein MM, Brügger OE, Janner SF, Kuchler U, Chappuis V, Jacobs R, et al. Indications and frequency for the use of cone beam computed tomography for implant treatment planning in a specialty clinic. *Int J Oral Maxillofac Implants* 2015; **30**: 1076–83. doi: https://doi.org/10.11607/jomi.4081
3. Corominas-Delgado C, Espona J, Lorente-Gascón M, Real-Voltas F, Roig M, Costa-Palau S. Digital implant impressions by cone-beam computerized tomography: a pilot study. *Clin Oral Implants Res* 2016; **27**: 1407–13. doi: https://doi.org/10.1111/clr.12754
4. Kang SR, Bok SC, Choi SC, Lee SS, Heo MS, Huh KH, et al. The relationship between dental implant stability and trabecular bone structure using cone-beam computed tomography. *J Periodontal Implant Sci* 2016; **46**: 116–27. doi: https://doi.org/10.5051/jpis.2016.46.2.116
5. McClammy TV. Endodontic applications of cone beam computed tomography. *Dent Clin North Am* 2014; **58**: 545–59. doi: https://doi.org/10.1016/j.cden.2014.03.004
6. Bayat S, Talaeipour AR, Sarlati F. Detection of simulated periodontal defects using cone-beam CT and digital intraoral radiography. *Dentomaxillofac Radiol* 2016; **45**: 20160030. doi: https://doi.org/10.1259/dmfr.20160030
7. Kapila SD, Nervina JM. CBCT in orthodontics: assessment of treatment outcomes and indications for its use. *Dentomaxillofac Radiol* 2015; **44**: 20140282. doi: https://doi.org/10.1259/dmfr.20140282
8. Wolff C, Mücke T, Wagenpfeil S, Kanatas A, Bissinger O, Deppe H. Do CBCT scans alter surgical treatment plans? Comparison of preoperative surgical diagnosis using panoramic versus cone-beam CT images. *J Craniomaxillofac Surg* 2016; **44**: 1700–5. doi: https://doi.org/10.1016/j.jcms.2016.07.025
9. Project S. *Radiation protection n°172: cone beam CT for dental and maxillofacial radiology*. Luxembourg: The British Institute of Radiology; 2012.
10. Scarfe WC, Li Z, Aboelmaaty W, Scott SA, Farman AG. Maxillofacial cone beam computed tomography: essence, elements and steps to interpretation. *Aust Dent J* 2012; **57**(Suppl 1): 46–60. doi: https://doi.org/10.1111/j.1834-7819.2011.01657.x
11. Parsa A, Ibrahim N, Hassam B, Van Der Stelt P, Wismeijer D. Influence of object location in cone beam computed tomography (NewTom 5G and 3G Accuitomo 170) on grey value measurements at an implant site. *Oral Radiol* 2014; **30**: 153–9.
12. Pauwels R, Jacobs R, Singer SR, Mupparapu M. CBCT-based bone quality assessment: are hounsfield units applicable? *Dentomaxillofac Radiol* 2015; **44**: 20140238. doi: https://doi.org/10.1259/dmfr.20140238
13. Makins SR. Artifacts interfering with interpretation of cone beam computed tomography images. *Dent Clin North Am* 2014; **58**: 485–95. doi: https://doi.org/10.1016/j.cden.2014.04.007

14. Schulze R, Heil U, Gross D, Bruellmann DD, Dranischnikow E, Schwanecke U, et al. Artefacts in CBCT: a review. *Dentomaxillofac Radiol* 2011; **40**: 265–73. doi: https://doi.org/10.1259/dmfr/30642039
15. Nagarajappa AK, Dwivedi N, Tiwari R. Artifacts: the downturn of CBCT image. *J Int Soc Prev Community Dent* 2015; **5**: 440–5. doi: https://doi.org/10.4103/2231-0762.170523
16. Iikubo M, Osano T, Sano T, Katsumata A, Ariji E, Kobayashi K, et al. Root canal filling materials spread pattern mimicking root fractures in dental CBCT images. *Oral Surg Oral Med Oral Pathol Oral Radiol* 2015; **120**: 521–7. doi: https://doi.org/10.1016/j.oooo.2015.06.030
17. Chang E, Lam E, Shah P, Azarpazhooh A. Cone-beam computed tomography for detecting vertical root fractures in endodontically treated teeth: a systematic review. *J Endod* 2016; **42**: 177–85. doi: https://doi.org/10.1016/j.joen.2015.10.005
18. Gaalaas L, Tyndall D, Mol A, Everett ET, Bangdiwala A. Ex vivo evaluation of new 2D and 3D dental radiographic technology for detecting caries. *Dentomaxillofac Radiol* 2016; **45**: 20150281. doi: https://doi.org/10.1259/dmfr.20150281
19. Siltanen S, Kolehmainen V, Järvenpää S, Kaipio JP, Koistinen P, Lassas M, et al. Statistical inversion for medical X-ray tomography with few radiographs: I. General theory. *Phys Med Biol* 2003; **48**: 1437–63. doi: https://doi.org/10.1088/0031-9155/48/10/314
20. Meilinger M, Schmidgunst C, Schütz O, Lang EW. Metal artifact reduction in cone beam computed tomography using forward projected reconstruction information. *Z Med Phys* 2011; **21**: 174–82. doi: https://doi.org/10.1016/j.zemedi.2011.03.002
21. Farman AG. Field of view. *Oral Surg Oral Med Oral Pathol Oral Radiol Endod* 2009; **108**: 477–8. doi: https://doi.org/10.1016/j.tripleo.2009.04.001
22. Pauwels R, Jacobs R, Bogaerts R, Bosmans H, Panmekiate S. Reduction of scatter-induced image noise in cone beam computed tomography: effect of field of view size and position. *Oral Surg Oral Med Oral Pathol Oral Radiol* 2016; **121**: 188–95. doi: https://doi.org/10.1016/j.oooo.2015.10.017
23. Hassan B, Couto Souza P, Jacobs R, de Azambuja Berti S, van der Stelt P, Souza PC. Influence of scanning and reconstruction parameters on quality of three-dimensional surface models of the dental arches from cone beam computed tomography. *Clin Oral Investig* 2010; **14**: 303–10. doi: https://doi.org/10.1007/s00784-009-0291-3
24. Oliveira ML, Freitas DQ, Ambrosano GM, Haiter-Neto F. Influence of exposure factors on the variability of CBCT voxel values: a phantom study. *Dentomaxillofac Radiol* 2014; **43**: 20140128. doi: https://doi.org/10.1259/dmfr.20140128
25. Scarfe WC, Farman AG, Sukovic P. Clinical applications of cone-beam computed tomography in dental practice. *J Can Dent Assoc* 2006; **72**: 75–80.
26. Spin-Neto R, Gotfredsen E, Wenzel A. Variation in voxel value distribution and effect of time between exposures in six CBCT units. *Dentomaxillofac Radiol* 2014; **43**: 20130376. doi: https://doi.org/10.1259/dmfr.20130376
27. Katsumata A, Hirukawa A, Okumura S, Naitoh M, Fujishita M, Ariji E, et al. Relationship between density variability and imaging volume size in cone-beam computerized tomographic scanning of the maxillofacial region: an in vitro study. *Oral Surg Oral Med Oral Pathol Oral Radiol Endod* 2009; **107**: 420–5. doi: https://doi.org/10.1016/j.tripleo.2008.05.049
28. Nishikawa K, Kousuge Y, Sano T. Is application of a quantitative CT technique helpful for quantitative measurement of bone density using dental cone-beam CT? *Oral Radiol* 2016; **32**: 9–13. doi: https://doi.org/10.1007/s11282-015-0202-z
29. Oliveira ML, Tosoni GM, Lindsey DH, Mendoza K, Tetradis S, Mallya SM. Assessment of CT numbers in limited and medium field-of-view scans taken using accuitomo 170 and veraviewepocs 3De cone-beam computed tomography scanners. *Imaging Sci Dent* 2014; **44**: 279–85. doi: https://doi.org/10.5624/isd.2014.44.4.279
30. Scarfe WC, Farman AG. What is cone-beam CT and how does it work? *Dent Clin North Am* 2008; **52**: 707–30. doi: https://doi.org/10.1016/j.cden.2008.05.005
31. Codari M, de Faria Vasconcelos K, Ferreira Pinheiro Nicolielo L, Haiter Neto F, Jacobs R, Vasconcelos KF. Quantitative evaluation of metal artifacts using different CBCT devices, high-density materials and field of views. *Clin Oral Implants Res* 2017; **28**: 1509–14. doi: https://doi.org/10.1111/clr.13019
32. Nardi C, Borri C, Regini F, Calistri L, Castellani A, Lorini C, et al. Metal and motion artifacts by cone beam computed tomography (CBCT) in dental and maxillofacial study. *Radiol Med* 2015; **120**: 618–26. doi: https://doi.org/10.1007/s11547-015-0496-2
33. Parsa A, Ibrahim N, Hassan B, van der Stelt P, Wismeijer D. Bone quality evaluation at dental implant site using multislice CT, micro-CT, and cone beam CT. *Clin Oral Implants Res* 2015; **26**: e1–e7. doi: https://doi.org/10.1111/clr.12315
34. Kuusisto N, Vallittu PK, Lassila LV, Huumonen S. Evaluation of intensity of artefacts in CBCT by radio-opacity of composite simulation models of implants in vitro. *Dentomaxillofac Radiol* 2015; **44**: 20140157. doi: https://doi.org/10.1259/dmfr.20140157
35. Pauwels R, Stamatakis H, Bosmans H, Bogaerts R, Jacobs R, Horner K, et al. Quantification of metal artifacts on cone beam computed tomography images. *Clin Oral Implants Res* 2013; **24**(Suppl A100): 94–9. doi: https://doi.org/10.1111/j.1600-0501.2011.02382.x